

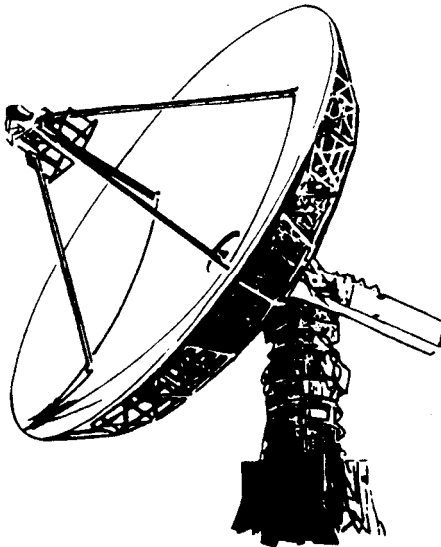
# **Design Principles and Test Methods for Low Phase Noise RF and Microwave Sources**

**Dieter Scherer**

**RF & Microwave  
Measurement  
Symposium  
and  
Exhibition**



**HEWLETT  
PACKARD**



## Introduction

In an increasing number of microwave applications such as satellite communications and modern radar, the system design requires signal sources with the lowest possible phase noise. The intent of this paper is to give an overview of considerations for the design and test of low phase noise sources. First, common definitions and specifications of frequency stability are shown and related to each other. Then design principles of low phase noise amplifiers, oscillators and phase noise characteristics of dividers are covered as well as their integration into crucial blocks of synthesized signal sources, phase lock loops, and reference multiplication. Finally, methods of measuring phase noise are compared.

### Terminology

$v(t) = V_s \cos [2\pi f_0 t + \Delta\phi(t)]$  represents a signal with a linearly growing phase component  $2\pi f_0 t$  and a randomly fluctuating term  $\Delta\phi(t)$ , phase noise.

Recall that  $f(t) = \frac{1}{2\pi} \frac{d\phi(t)}{dt}$ . Therefore, we can talk in terms of phase fluctuations or in terms of frequency fluctuations to describe one and the same signal.

Some conventional terms for characterizing frequency stability in the time domain are: (see Fig. 1a)

- Long term stability, describing slow changes of frequency like aging.
- Short term stability, covering frequency noise and fluctuations with random periods shorter than some minutes.

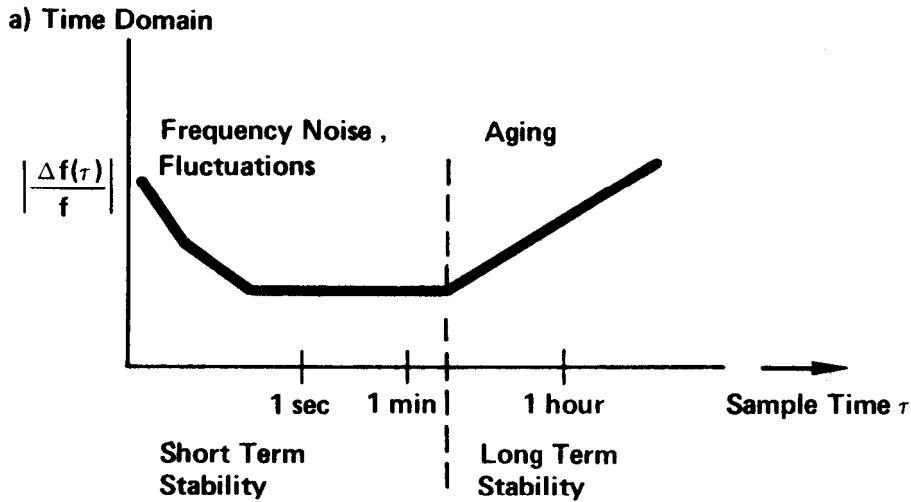


Fig. 1a shows the fractional frequency deviation plotted over sample time  $\tau$ .

Likewise, in the frequency domain, terms like Random Walk, Flicker and White Phase Noise describe the slope of spectral density. Fig. 1b plots the spectral density distribution of phase fluctuation. The Fourier Frequency (here labeled  $f_m$ ) may also be called Sideband Frequency, Offset Frequency, Modulation Frequency or Baseband Frequency.

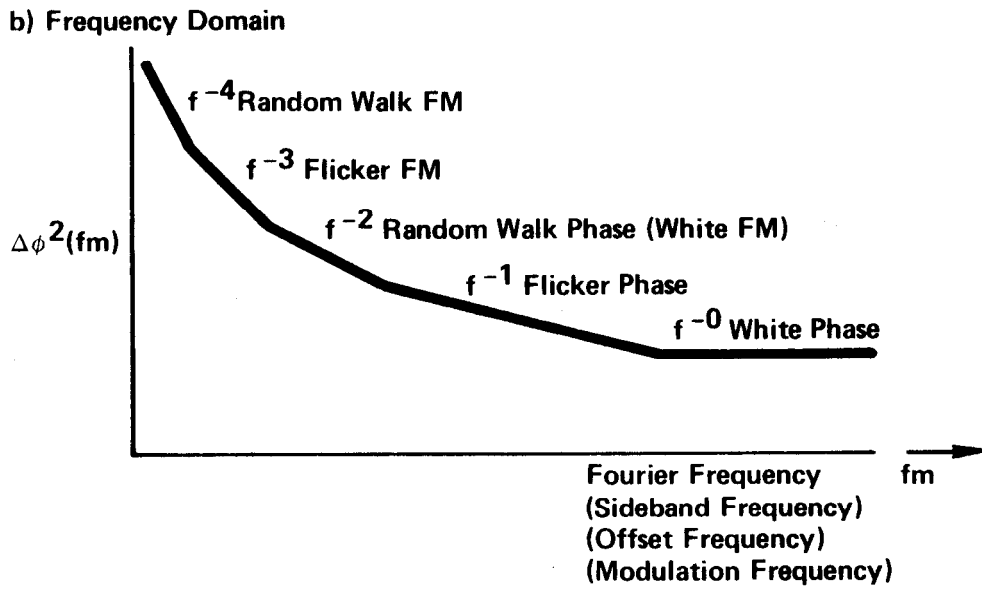


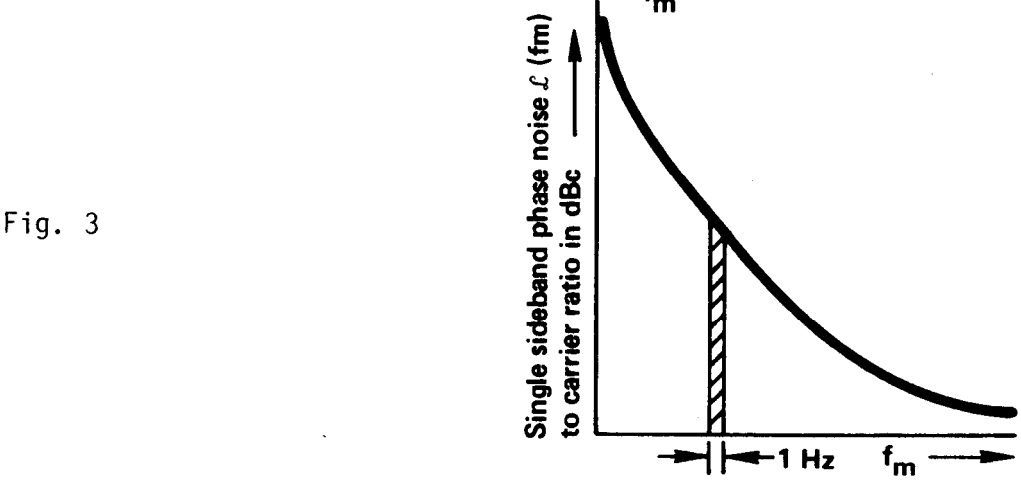
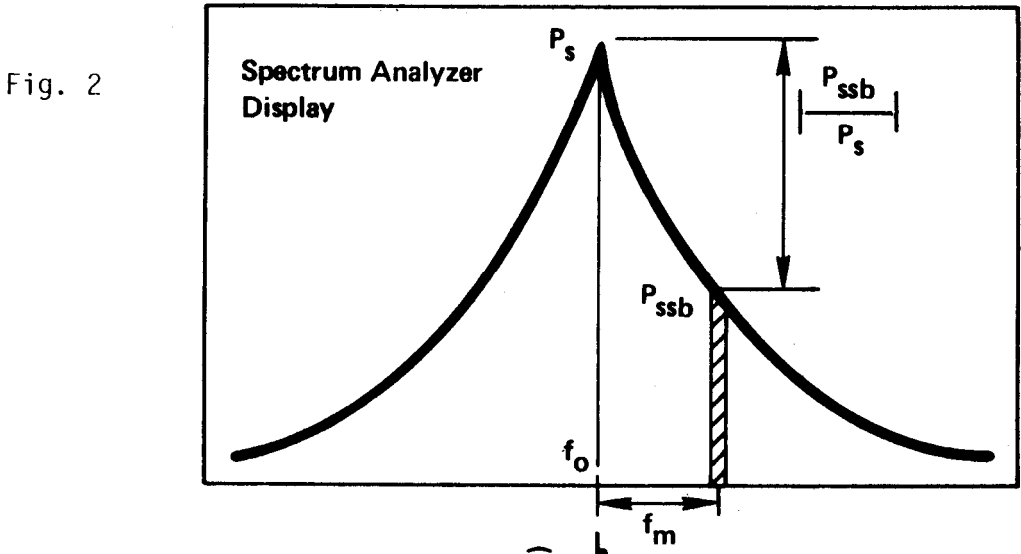
Fig. 1b

Definition of  $\mathcal{L}(f_m)$

The most common characterization of phase noise of sources in the frequency domain is the RF power spectrum, probably because this is what one observes on a spectrum analyzer when AM noise is insignificant (Fig. 2).

The display is symmetrical. Taking just one side and looking at sideband noise in a 1Hz bandwidth leads to the definition of script  $\mathcal{L}(f_m)$ :

Script  $\mathcal{L}(f_m)$  is defined as the ratio of the single sideband power of phase noise in a 1Hz bandwidth  $f_m$  Hertz away from the carrier frequency to the total signal power.



How Does Phase Modulation Relate to  $\mathcal{L}$ ?

The previous definition of  $\mathcal{L}$  is primarily applied to random noise. To relate  $\mathcal{L}$  to random or sinusoidal phase modulation, a signal with sinusoidal frequency modulation is considered first and converted to phase modulation.

$$f = f_o + \Delta f_{\text{peak}} \cos 2\pi f_m t$$

$$\phi = \int 2\pi f(t) dt$$

$$\phi = 2\pi f_o t + \frac{\Delta f_{\text{peak}}}{f_m} \sin 2\pi f_m t$$

$$\phi = 2\pi f_o t + \Delta\phi_{\text{peak}} \sin 2\pi f_m t$$

$$v(t) = V_s \cos \left( 2\pi f_o t + \frac{\Delta f_{\text{peak}}}{f_m} \sin 2\pi f_m t \right)$$

Bessel algebra yields the single sideband to carrier ratio. For a small modulation index,  $\Delta\phi_{\text{peak}} \ll 1$ , the following approximation holds:

$$\frac{V_{\text{ssb}}}{V_s} \approx J_1 \left( \frac{\Delta f_{\text{peak}}}{f_m} \right) \approx \frac{1}{2} \frac{\Delta f_{\text{peak}}}{f_m} \approx \frac{1}{2} \Delta\phi_{\text{peak}}$$

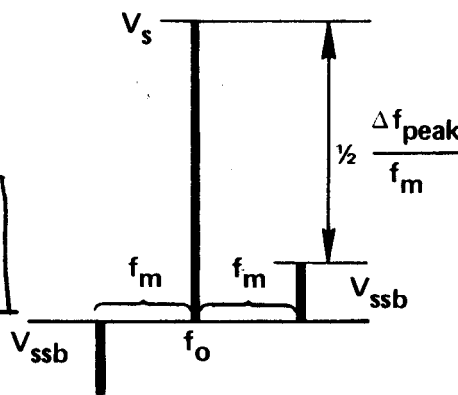


Fig. 4

or in logarithmic form:

$$\left( \frac{V_{\text{ssb}}}{V_s} \right)^2 = -6\text{dB} + 20 \log \Delta\phi_{\text{peak}}$$

For random phase fluctuations,  $\Delta\phi_{\text{peak}}$  is replaced with an equivalent  $\sqrt{2} \Delta\phi_{\text{rms}}$  for a 1Hz bandwidth.

$$\mathcal{L}(f_m) = \left( \frac{V_{\text{SSB}}}{V_s} \right)_{1\text{Hz}}^2 = \frac{1}{4} (\sqrt{2} \Delta\phi_{\text{rms}})^2 = \frac{1}{2} \Delta\phi_{\text{rms}}^2$$

Or inversely, the Spectral Density of Phase Noise expressed by  $\mathcal{L}$  :

$$S_{\Delta\phi}(f_m) = \Delta\phi_{\text{rms}}^2 = 2 \mathcal{L}(f_m)$$

$$S_{\Delta\phi}(f_m) \Big|_{\text{dB}} = 3\text{dB} + \mathcal{L}(f_m) \Big|_{\text{dBc}}$$

Spectral Density of Frequency Fluctuations, Related to  $S_{\Delta\phi}$  and  $\mathcal{L}$

Stability measurements with frequency discriminators give the Spectral Density of Frequency Fluctuations.

$$S_{\Delta f}(f_m) = \Delta f_{\text{rms}}^2$$

To relate the spectral density of frequency fluctuations to the spectral density of phase noise we recall that

$$\Delta f(t) = \frac{1}{2\pi} \frac{d\Delta\phi(t)}{dt}$$

Transformed into the frequency domain:

$$\Delta f(f_m) = f_m \Delta\phi(f_m)$$

$$S_{\Delta f}(f_m) = \Delta f_{\text{rms}}^2(f_m) = f_m^2 S_{\Delta\phi}(f_m) = 2f_m^2 \mathcal{L}(f_m)$$

NBS proposes to standardize the spectral density of fractional frequency fluctuations. The instantaneous frequency deviation is normalized to the carrier frequency  $f_0$ .

$$y(t) = \frac{\Delta f(t)}{f_0}$$

$$S_y(f_m) = \frac{1}{f_0^2} \quad S_{\Delta f}(f_m) = \frac{f_m^2}{f_0^2} \quad S_{\Delta\phi}(f_m) = \frac{2f_m^2}{f_0^2} \quad \mathcal{L}(f_m)$$

Characterizing fractional frequency fluctuations allows better comparison between sources with different carrier frequencies.

Residual FM Related to  $\mathcal{L}(f_m)$

Residual FM is another common way to specify the frequency stability of signal generators. Residual FM is the total rms frequency deviation within a specified bandwidth. Commonly used bandwidths are 50Hz to 3kHz, 300Hz to 3kHz, 20Hz to 15kHz.

$$\Delta f_{res} = \sqrt{2} \sqrt{\int_a^b \mathcal{L}(f_m) f_m^2 df_m}$$

The table below correlates  $\Delta f_{res}$  and  $\mathcal{L}(f_m)$  for specific slopes of  $\mathcal{L}(f_m)$  and  $\mathcal{L} @ 1\text{kHz} = -100\text{dBc}$ .

$\mathcal{L}^* @ 1 \text{ kHz}$ [dBc]	Slope of $\mathcal{L}(f_m)$		Residual FM $\Delta f_{res}$ [Hz]		
	Exponent	dB/oct	50 Hz to 3 kHz	300 Hz to 3 kHz	20 Hz to 15 kHz
-100	0	0 dB	1.34	1.34	15.0
-100	-1	-3 dB	.95	.94	4.74
-100	-2	-6 dB	.77	.73	1.73
-100	-3	-9 dB	.90	.68	1.15



\*For any  $\mathcal{L}$  @ 1 kHz different to  $-100$  dBc multiply

$$\Delta f_{\text{res}} \text{ of the table by antilog } \frac{100 - |\mathcal{L} @ 1 \text{ kHz/dBc}|}{20}$$

The table does not take into account any microphonic or spurious sidebands.

Example:

$\mathcal{L}$  @ 1 kHz =  $-88$  dBc, Slope  $-9$  dB

For bandwidth 20 Hz to 15 kHz:

$$\Delta f_{\text{res}} = 1.15 \text{ Hz} \times \text{antilog } \frac{100 - 88}{20} = 4.6 \text{ Hz}$$

### Allan Variance Related to $\mathcal{L}(f_m)$

For many applications, like high stability crystal oscillators or doppler radar systems, it is more relevant to describe frequency stability in the time domain. The characterization is based on the sample variance of fractional frequency fluctuations. Averaging differences of consecutive sample pairs with no dead-time inbetween yields the Allan Variance,  $\sigma_y^2(\tau)$ , which is the proposed standard measure of frequency stability.

$$\sigma_y^2(\tau) = \frac{1}{2(M-1)} \sum_{K=1}^{M-1} (\bar{y}_{K+1} - \bar{y}_K)^2$$

$\bar{y}_k$  is the average fractional frequency difference of the k-th sample measured over sample time  $\tau$ .

Conversions from frequency to time domain data and vice versa are possible but tedious. The power spectrum  $\mathcal{L}(f_m)$  needs to be approximated by integer slopes of 0, -1, -2, -3, -4. Then conversion formulas (see Table below) can be applied. A good description of this procedure is given in [2] and [5].

Conversion Table

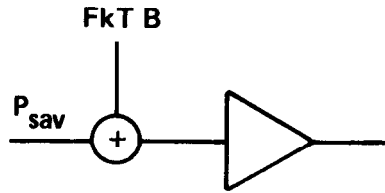
	<u>Slope of <math>\sigma_y^2(\tau)</math></u>	<u><math>\sigma_y(\tau) =</math></u>	<u><math>\mathcal{L}(f) =</math></u>	<u>Slope of <math>\mathcal{L}(f)</math></u>
WHITE PHASE	-2	$\frac{\sqrt{\mathcal{L}(f) f_h}}{2.565 f_o} \tau^{-1}$	$\frac{(a_y(\tau) \tau f_o (2.565))^2}{f_h} f^0$	0
FLICKER PHASE	-1.9	$\frac{\sqrt{\mathcal{L}(f) f (2.184 + \ln(f_h \tau))}}{2.565 f_o} \tau^{-1}$	$\frac{(a_y(\tau) \tau f_o (2.565))^2}{2.184 + \ln(f_h \tau)} f^{-1}$	-1
WHITE FREQ.	-1	$\frac{\sqrt{\mathcal{L}(f) f^2}}{f_o} \tau^{-1/2}$	$(a_y(\tau) \tau^{1/2} f_o)^2 f^{-2}$	-2
FLICKER FREQ.	0	$\frac{1.665 \sqrt{\mathcal{L}(f) f^3}}{f_o} \tau^0$	$0.361 (a_y(\tau) f_o)^2 f^{-3}$	-3
RANDOM WALK FREQ.	+1	$\frac{3.63 \sqrt{\mathcal{L}(f) f^4}}{f_o} \tau^{1/2}$	$(0.276 a_y(\tau) \tau^{-1/2} f_o)^2 f^{-4}$	-4

$\tau$  = measurement time,  $y = \Delta f_o/f_o$ ,  $f_o$  = carrier,  $f$  = sideband frequency,  $f_h$  = measurement system bandwidth

We have covered the most frequently used measures of phase noise and have inter-related them. Next we take a look at the generation of phase noise in amplifiers and oscillators.

Phase Noise Caused by Additive Noise

Let us examine how phase noise is added to a signal passing through an amplifier with noise figure F.



The power spectrum of white noise added to the signal can be thought of as the sum of 1Hz bands each of which has the available power of FkT. Each band is now replaced by a discrete signal  $V_{n\text{ rms}}$  of equivalent available power:

$$V_{n\text{ rms}} = \sqrt{\frac{FkT}{R}}$$

The phasor diagram in Fig. 5c reveals the phase perturbation  $\Delta\theta_{\text{peak}}$ , caused by  $V_{n\text{ rms}}$ .

For small  $\Delta\theta$ ,

$$\Delta\theta_{\text{peak } 1} = \frac{V_{n\text{ rms } 1}}{V_{s\text{ av rms}}} = \sqrt{\frac{FkT}{P_{s\text{ av}}}}$$

$$\Delta\theta_{1\text{ rms}} = \frac{1}{\sqrt{2}} \sqrt{\frac{FkT}{P_{s\text{ av}}}}$$

At  $f_0 - f_m$  another noise signal of equal magnitude but with random phase relation to the noise signal at  $f_0 + f_m$  causes the same phase fluctuation of the signal.

Both  $\Delta\theta_{\text{rms}}$  add powerwise and result in a total

$$\Delta\theta_{\text{rms total}} = \sqrt{\frac{FkT}{P_{s\text{ av}}}}$$

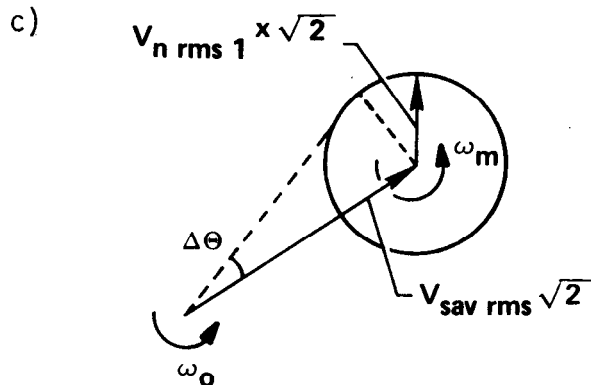
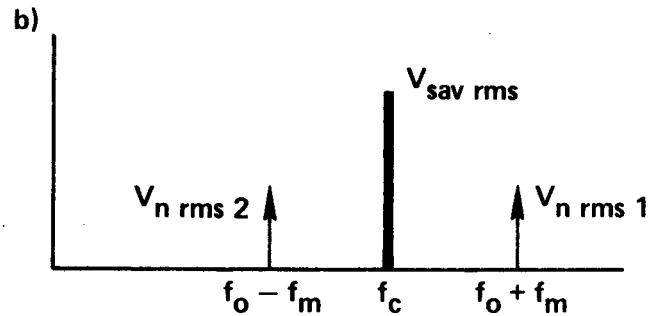
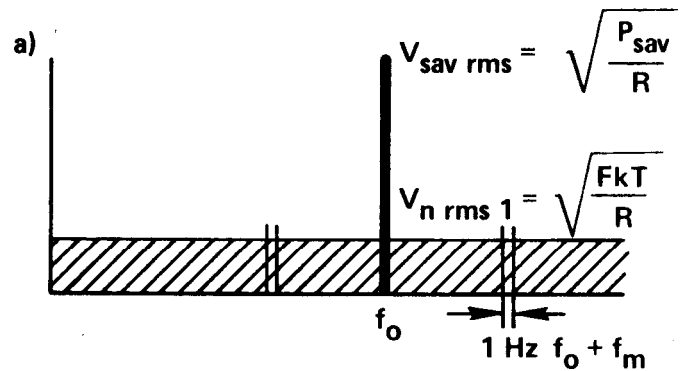


Fig. 5

The spectral density of phase noise is therefore:

$$S_{\Delta\theta} = \Delta\theta_{\text{rms}}^2 = \frac{FkT}{P_{s \text{ av}}}$$

$$\mathcal{L} = \frac{1}{2} \frac{FkT}{P_{s \text{ av}}}$$

Using available signal and noise power assumed a matched input. But the same signal-to-noise ratio and therefore the same phase noise results with mismatched input, assuming  $F$  remains unchanged.

Example: A signal of 0dBm passing through an amplifier with 5dB noise figure should have a spectral density of phase noise of

$$S_{\Delta\theta} = -174\text{dBm} + 5\text{dB} - 0\text{dBm} = -169\text{dB}$$

This theoretical floor can be observed only at some offset. With a practical transistor amplifier,  $S_{\Delta\theta}$  shows a flicker characteristic which is empirically described by the corner frequency  $f_c$ . For Fourier frequencies below  $f_c$ ,  $S_{\Delta\theta}$  increases with  $f_m^{-1}$ .

$f_c$  is very device-dependent and can range from 1kHz to 1MHz. It is caused by low frequency device noise modulating the phase of the passing signal by modulating the transconductance and the input and output impedances of the amplifier. Upconversion of the low frequency device noise has the same cause, the non-linear parameters of the device. The effect of this multiplicative process can be reduced by:

1. Negative feedback at low frequency.
2. Some negative feedback at RF frequency to stabilize the transconductance.
3. Designing the RF amplifier for low noise figure also at low frequency.

Actual Phase Noise

$$S_{\Delta} = \frac{FkT}{P_{sav}} \left( 1 + \frac{f_c}{f_m} \right)$$

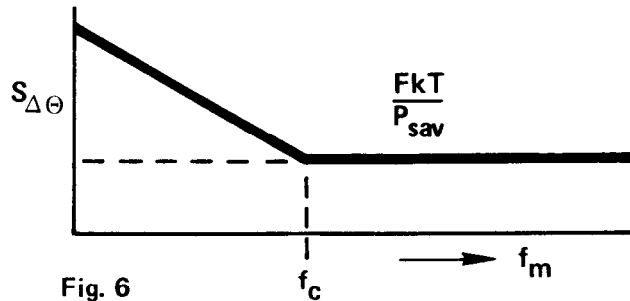
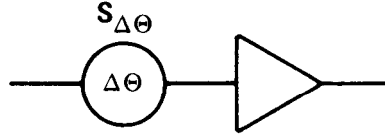


Fig. 6

$S_{\Delta\theta}$  including the empirical modification due to low frequency device noise is modeled in Fig. 6 and will be used as the phase noise stimulus in the following model of a feedback oscillator.

Leeson's Model of Phase Noise in Oscillators

Leeson's model of a feedback oscillator describes phase noise in free running oscillators [8]. It consists of an amplifier with noise figure F and a filter, e.g. a resonator in the feedback loop. Ref. [9] describes a more general model.

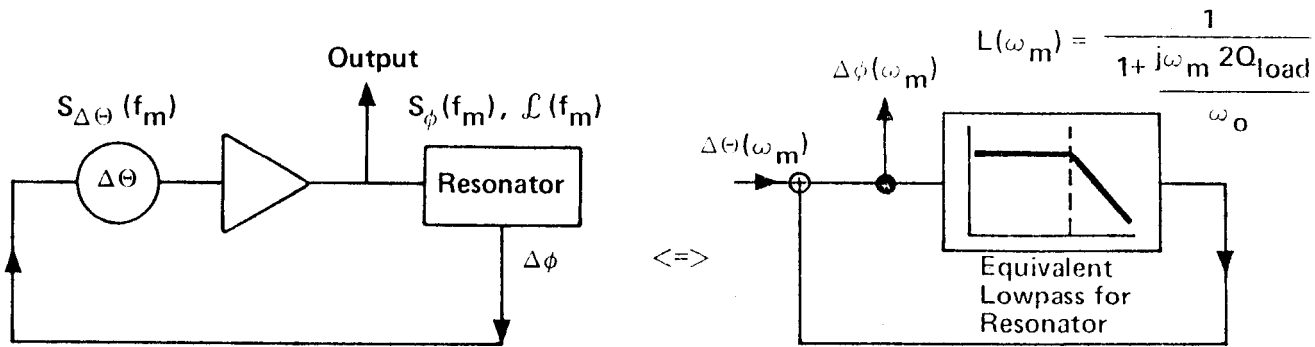


Fig. 7

Fig. 7 shows how this model transfers into a phase feedback loop. Transmission theory states that the transfer function of a phase modulated RF signal passing through a bandpass equals the transfer function of the modulating signal passing through an equivalent lowpass.

A tank circuit as a bandpass results in the following lowpass transfer function:

$$L(\omega_m) = \frac{1}{1 + j \frac{\omega_m 2Q_{load}}{\omega_0}}$$

with  $\frac{\omega_0}{2Q_{load}}$  representing the half bandwidth of the resonator.

Physically interpreted, the phase modulation is transferred unattenuated through the resonator up to rates equal to half of its bandwidth. As the modulation rate increases further, the resonator attenuates the passing phase modulation with 6dB per octave.

The closed loop response of the phase feedback loop due to a stimulus  $\Delta\theta(\omega_m)$  is

$$\Delta\phi(\omega_m) = \left(1 + \frac{\omega_o}{j\omega_m 2Q_{load}}\right) \Delta\theta(\omega_m)$$

Its power transfer function equals

$$S_\phi(f_m) = \left[1 + \frac{1}{f_m^2} \left(\frac{f_o}{2Q_{load}}\right)^2\right] \times S_{\Delta\theta}(f_m)$$

Phase Transfer Function
Phase Perturbation

$$\mathcal{L}(f_m) = \frac{1}{2} \left[1 + \frac{1}{f_m^2} \left(\frac{f_o}{2Q_{load}}\right)^2\right] S_{\Delta\theta}$$

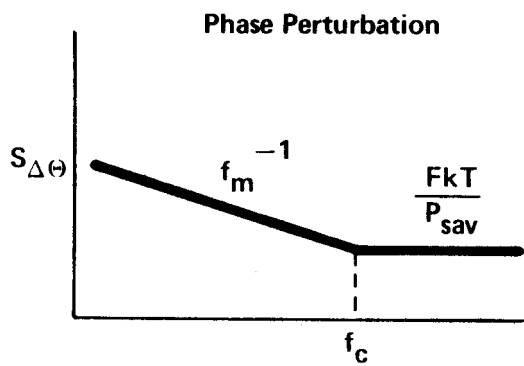
$$S_{\Delta\theta} = \frac{FkT}{P_{s av}} \left(1 + \frac{f_c}{f_m}\right)$$

This equation describes phase noise at the output of the amplifier. It illustrates how  $S_{\Delta\theta}$ , the phase perturbation at the input of the amplifier, is enhanced by the positive phase feedback within the half bandwidth of the resonator,  $\frac{f_o}{2Q_{load}}$ .

Depending on the relation of the corner frequency of flicker noise,  $f_c$ , in  $S_{\Delta\theta}$  to the half bandwidth of the resonator, two characteristic phase noise distributions result from multiplying the transfer function with the perturbation. They are depicted in Fig. 8.

### High Q Oscillator

$$\frac{f_o}{2Q} < f_c$$



### Low Q Oscillator

$$\frac{f_o}{2Q} > f_c$$

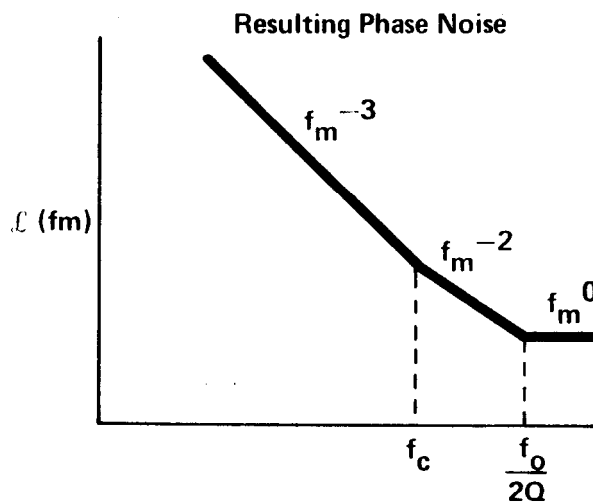
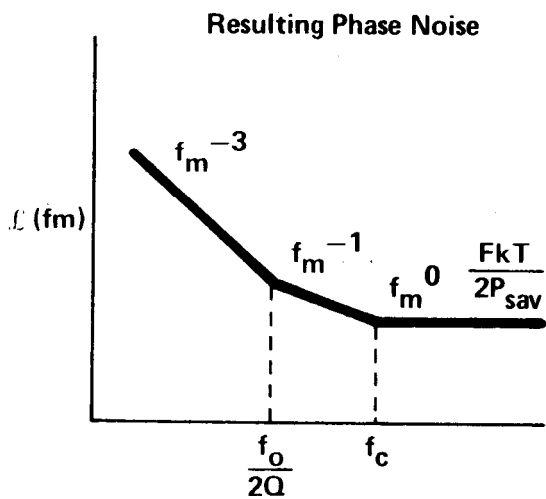
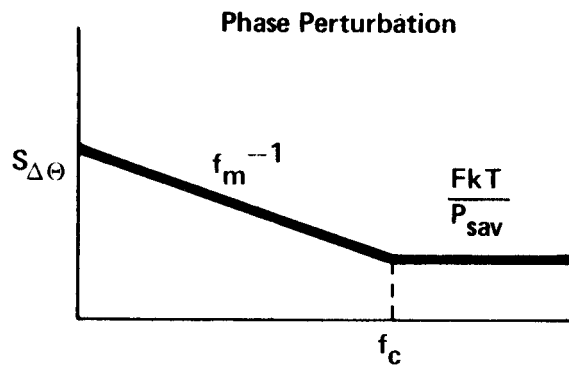


Fig. 8



Optimization of Phase Noise in Oscillators

Let us expand Leeson's equation to expose the various parameters of an actual oscillator which are relevant to phase noise optimization. We focus on  $\mathcal{L}(f_m)$  within the half bandwidth of the resonator:

$$\text{for } f_m < \frac{f_o}{2Q_{\text{load}}}$$

$$\mathcal{L}(f_m) = \frac{1}{2} \frac{1}{\omega_m^2} \left( \frac{\omega_o}{2Q_{\text{load}}} \right)^2 \frac{FkT}{P_{s \text{ av}}} \left( 1 + \frac{f_c}{f_m} \right)$$

Typical Oscillator

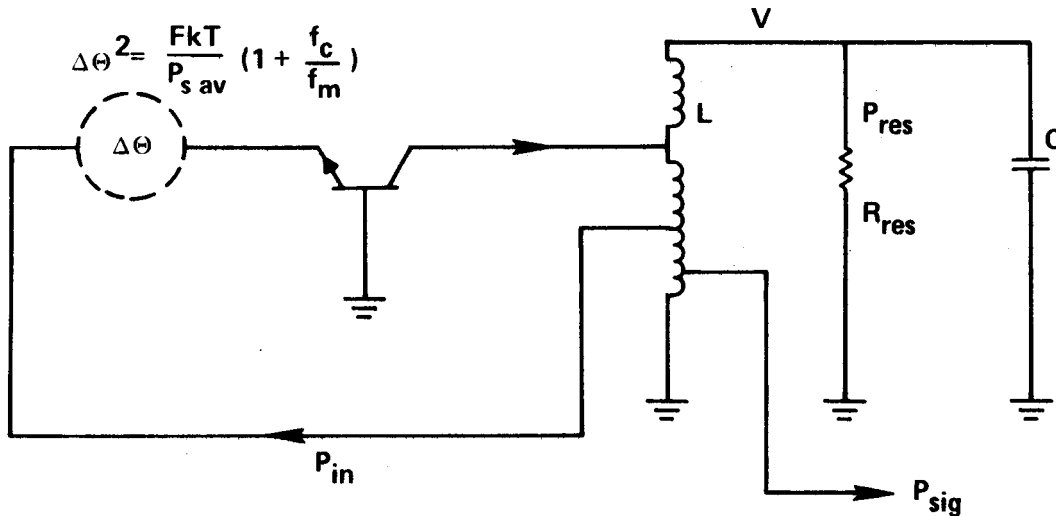


Fig. 9

$Q_{\text{load}}$  can be expressed as:

$$Q_{\text{load}} = \frac{\omega_o W_e}{P_{\text{diss, total}}} = \frac{\omega_o W_e}{P_{\text{in}} + P_{\text{res}} + P_{\text{sig}}} = \frac{\text{Reactive power}}{\text{Total dissipated power}}$$

where  $W_e$  is the reactive energy going between L and C

$$W_e = \frac{1}{2} CV^2 \quad P_{\text{res}} = \frac{\omega_o W_e}{Q_{\text{unl}}}$$

$$L(\omega_m) = \frac{1}{8} \frac{FkT}{P_{s\ av}} \frac{\omega_o^2}{\omega_m^2} \left( \frac{P_{in}}{\omega_o W_e} + \frac{1}{Q_{unl}} + \frac{P_{sig}}{\omega_o W_e} \right)^2 \left( 1 + \frac{\omega_c}{\omega_m} \right)$$

The diagram shows the equation for phase noise  $L(\omega_m)$  enclosed in a box. Below this box, five smaller boxes are connected by lines to specific parts of the equation:
 

- Phase Perturbation** points to the  $\frac{1}{8} \frac{FkT}{P_{s\ av}}$  term.
- Resonator Q** points to the  $\frac{1}{Q_{unl}}$  term.
- Flicker Effect** points to the  $\left( 1 + \frac{\omega_c}{\omega_m} \right)$  term.
- Input Power over Reactive Power** points to the  $\frac{P_{in}}{\omega_o W_e}$  term.
- Signal Power over Reactive Power** points to the  $\frac{P_{sig}}{\omega_o W_e}$  term.

This equation is particularly significant because it encompasses most of the causes of phase noise in oscillators. Minimization of phase noise dictates the following design rules:

- Maximize the unloaded Q
- Maximize the reactive energy by means of a high RF voltage V across the resonator and a high capacitance C. The limits are set by breakdown voltages of the active device and varactor and by the forward bias condition of the varactor.
- Limiting should occur without degradation of Q. A two-stage amplifier, e.g., isolates the limiting port from the resonator. Forward bias of the varactor due to high RF voltage should be avoided.
- Choose an active device with low noise figure F. F is the noise figure in the actual impedance environment the device sees.

In many applications it is preferable to deal with equivalent noise voltage and noise current since they are independent of the source impedance. In the example of Figure 9, the amplifier input is coupled into the resonator. Therefore the source impedance changes drastically as a function of the offset frequency.

- Minimize phase perturbation given by the ratio of additive noise to the lowest signal level. In the switched reactance oscillator, Figure 15, the high input impedance of the two-stage FET amplifier allows the input power to be neglected.  $\frac{FkT}{P_{s\ av}}$  can be replaced with the ratio of noise voltage to signal voltage at

the limiting port  $\left(\frac{V_n}{V_{SL}}\right)^2$ . Obviously, the limited signal voltage,  $V_{SL}$ , should be maximal.

- Choose an active device with low flicker noise.
- Minimize the effect of flicker noise which modulates transconductance, input and output impedances of the active device by low frequency feedback and proper bias. The effect of modulated input and output impedance can further be minimized by maximizing the stable tank circuit capacitance as was previously advocated for a different reason.
- Minimize the signal power taken out without going below the limits set by additive noise.
- Couple the signal power of the resonator so that there is a continuing drop of phase noise beyond the half bandwidth of the resonator.

These design principles were applied in the 310 to 640MHz VCO of Figure 15. As an example let us calculate the phase noise performance of this VCO at 500MHz and at 100KHz offset.

The input power of the two-stage FET amplifier can be neglected. The phase perturbation  $\frac{FkT}{P_{sav}} \left(1 + \frac{\omega_c}{\omega_m}\right)$  is replaced by the noise voltage to signal ratio at the input of the 2nd stage, the limiting port.

For a 2N5397  $V_n = 6nV$  (accounts for both FET's)  
 $V_{SL} = 1V$   
 $C = 23pF$   
 $V = 10V$   
 $Q_{unl} = 200$   
 $P_{sig} = 4mW$   
 $f_o = 500MHz$

$$\mathcal{L} @ 100kHz = \frac{1}{8} \left(\frac{6 \times 10^{-9}}{1}\right)^2 \left(\frac{5 \times 10^8}{10^5}\right)^2 \left(\frac{1}{200} + \frac{.004}{2\pi \times 5 \times 10^8 \times .5 \times 23 \times 10^{-12} \times 10^2}\right)^2$$

$$\mathcal{L} @ 100kHz = -144dBc$$

The actual oscillator measured -142dBc.

Fig. 10 shows the phase noise performance of some free-running oscillators designed with low phase noise as a primary goal. Of course, the curves cannot be compared directly with each other since they not only differ in RF frequencies but also have quite different objectives in terms of tunability.

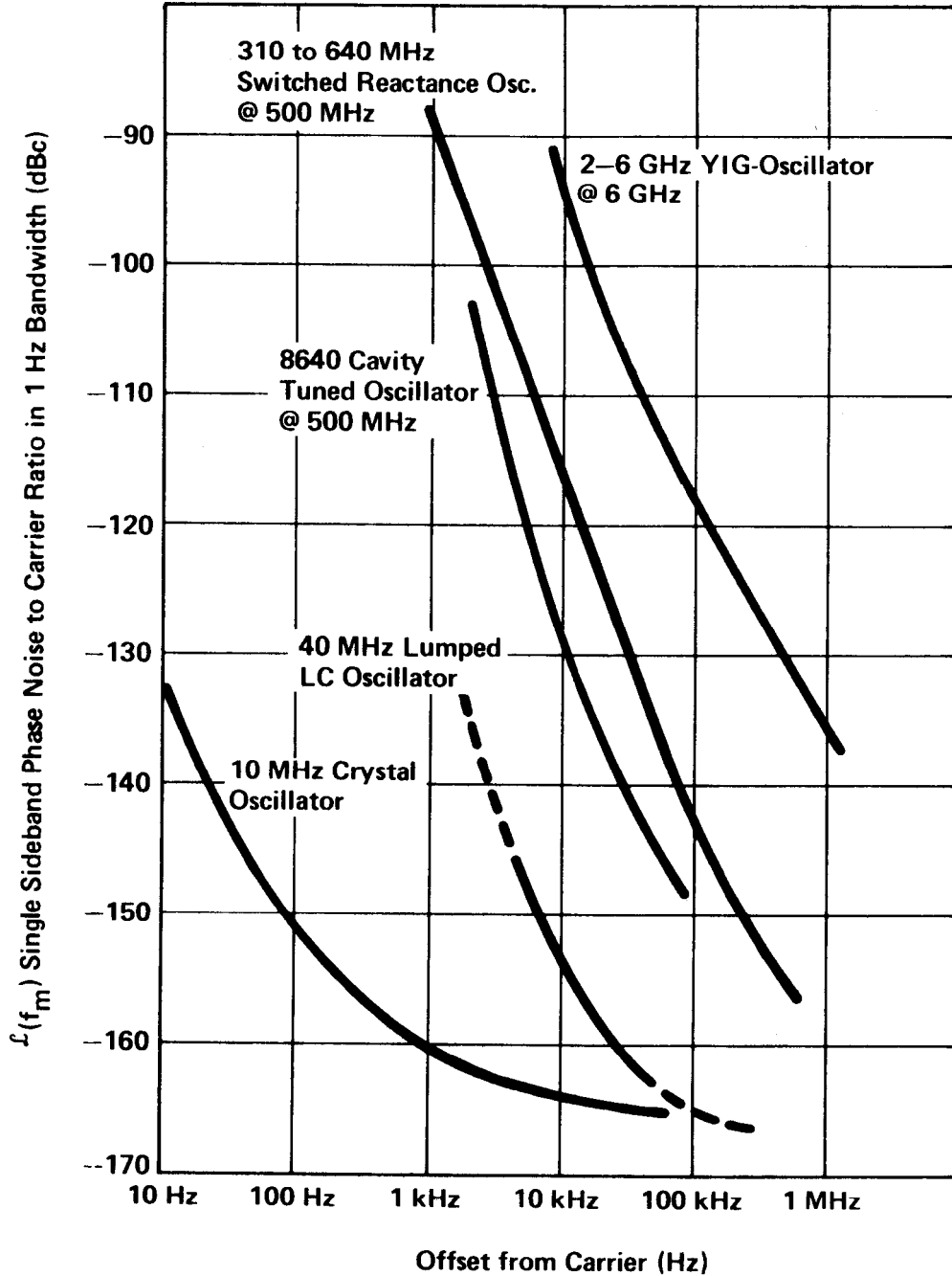


Fig. 10

### Phase Noise Characteristics of Dividers

Before analyzing the phase noise performance of phase locked sources, let us consider phase noise introduced by frequency dividers. As the next paragraph will point out, they may be the limiting component in a phase lock loop. They also play a key role in direct frequency synthesis.

Phase noise at the input of the divider appears at the divider output reduced by N. In the residual phase noise measurement of Fig. 11 this input (source) noise contribution cancels and only phase noise generated by the divider is measured. Phase noise data refer to the divided-down signal. A phase noise floor of -150 to -160dBc is typical for ECL devices. The considerably lower floor of TTL dividers is measureable only if care is taken to avoid sampling effects.

### Examples of Phase Noise Introduced by Dividers

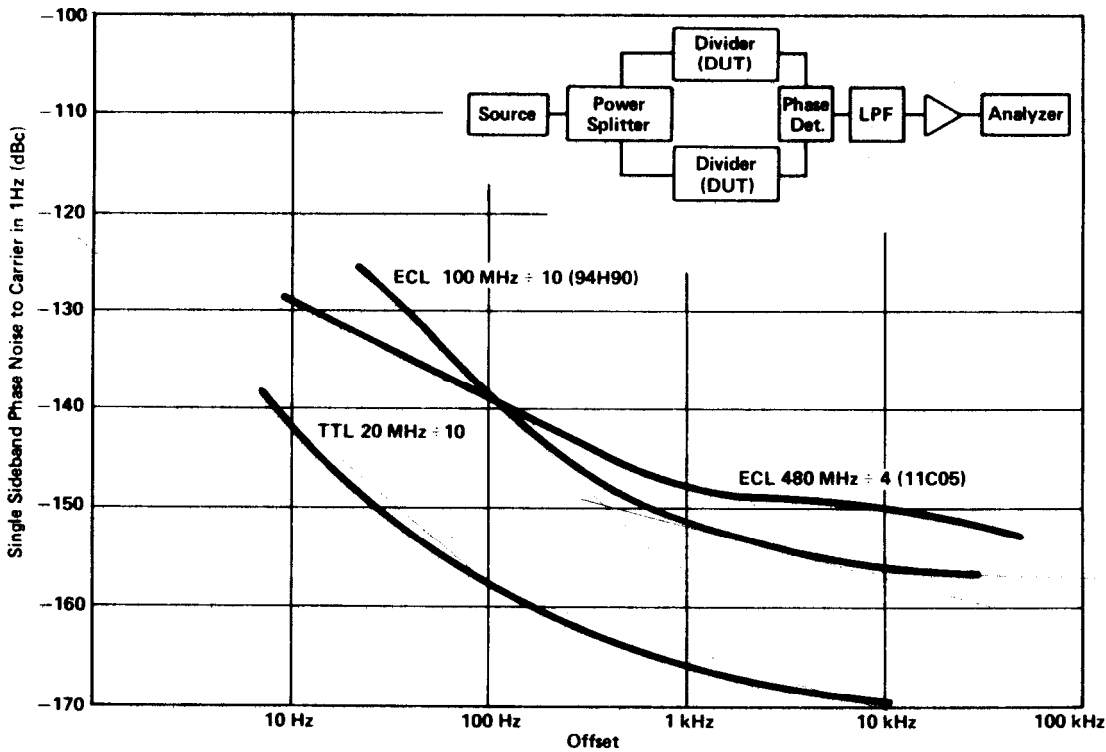


Fig. 11

Noise Considerations for Phase-Locked Sources

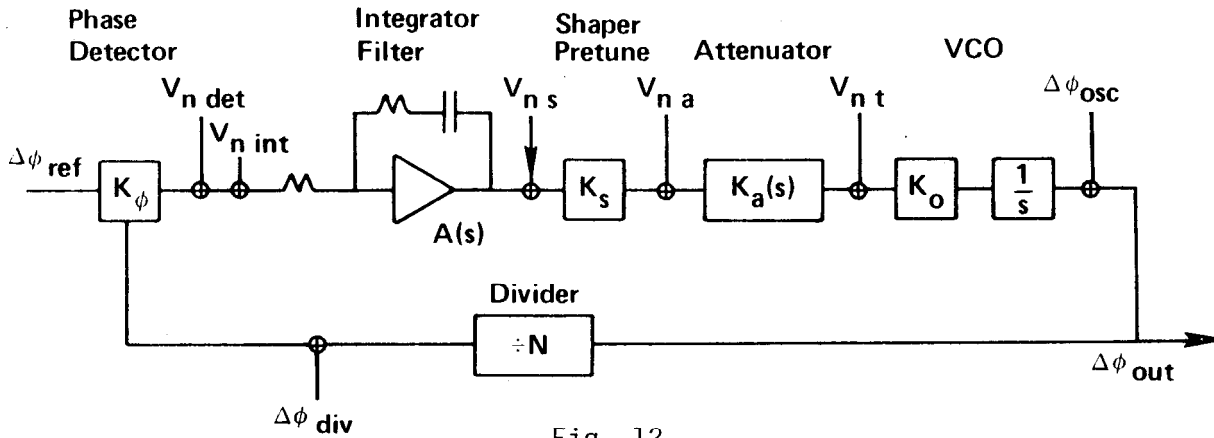


Fig. 12

Fig. 12 shows a typical phase-lock loop (PLL) - typical with the exception of the attenuator at the oscillator tuning port. This attenuator is justified in the following design rules. The objective is to minimize  $\Delta\phi_{out}$  due to any noise input. The following design rules emerge when we look at respective transfer functions:

- Minimize phase noise of the free running VCO

$$\frac{\Delta\phi_{out}}{\Delta\phi_{osc}} = \frac{1}{1 + G_{ol}(s)}$$

$G_{ol}(s)$  is the open loop gain:

$$G_{ol}(s) = K_{\phi} A(s) K_s K_a(s) K_o \frac{1}{N} \frac{1}{s}$$

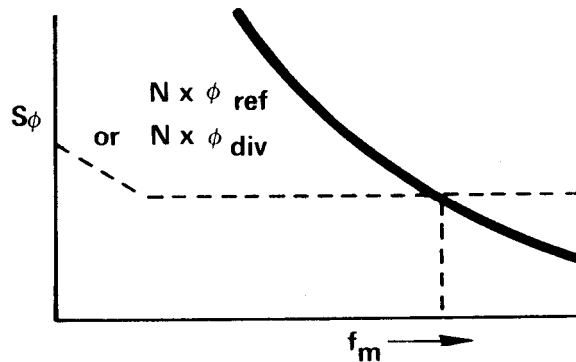


Fig. 13

Phase noise of the free running oscillator is reduced by the loop gain. This leads to the next rule.

- Maximize bandwidth and open-loop gain. The bandwidth is limited by a number of constraints. By comparing phase noise of the free-running VCO with phase noise contributions from the reference source, the divider output, and the phase detector, the bandwidth is determined.

All 3 phase noise sources have the same transfer function:

$$\frac{\Delta\phi_{\text{out}}}{\Delta\phi_{\text{ref}}} = \frac{N}{1 + \frac{1}{G_{\text{ol}}(s)}}$$

Maximizing the loop bandwidth makes sense only as long as reference noise (or divider noise, or phase detector noise) multiplied by N does not exceed the phase noise of the free-running VCO.

Other considerations, such as the filtering of the reference signal or spurious on the reference signal and loop stability, can determine the choice of the bandwidth.

- Avoid dividers if possible. As noted above, they cause multiplication by N of the reference, phase detector, and divider output phase noise.
- Minimize integrator, shaper and attenuator noise. The choice of impedance levels and pretune filtering might be constrained by switching speed considerations.
- Maximize phase detector gain  $K_{\phi}$ .  
Any noise input following the phase detector is reduced by  $\frac{1}{K_{\phi}}$ .

$$\frac{\Delta\phi_{\text{out}}}{V_{\text{n int}}} = \frac{1}{K_{\phi}} \frac{N}{1 + \frac{1}{G_{\text{ol}}(s)}}$$

- Minimize the sensitivity,  $K_o$  [MHz/V], of the VCO. Given a chosen bandwidth, phase noise due to  $V_{\text{ns}}$ ,  $V_{\text{na}}$ , and  $V_{\text{nt}}$  is proportional to  $K_o$ .

$$\frac{\Delta\phi_{\text{out}}}{V_{\text{nt}}} = \frac{\frac{K_o}{S}}{1 + G_{\text{ol}}(s)}$$

- Employ an attenuator and minimize  $K_a(s)$ . Again, given a chosen bandwidth, noise inputs preceding the attenuator are reduced by  $K_a(s)$ . This holds also for noise outside the loop bandwidth. For example, phase noise outside the loop bandwidth caused by  $V_{ns}$  amounts to:

$$\Delta\phi_{out} = K_a(s) K_s K_o \frac{1}{s} V_{n \text{ int}}$$

The attenuator is usually a lead-lag network.

The following equation sums up all the phase noise contributions.

$$\begin{aligned} \Delta\phi_{out}^2(s) &= \left( \frac{N}{1 + \frac{1}{G_{ol}(s)}} \right)^2 \left[ \Delta\phi_{ref}^2(s) + \Delta\phi_{div}^2(s) \right] \\ &+ \frac{1}{K_\phi^2} \left( \frac{N}{1 + \frac{1}{G_{ol}(s)}} \right)^2 \left[ V_{n \text{ det}}^2(s) + V_{n \text{ int}}^2(s) + \frac{1}{A(s)^2} V_{ns}^2(s) + \frac{1}{A(s)^2} \frac{1}{K_s^2} V_{na}^2(s) \right] \\ &+ \left( \frac{1}{1 + G_{ol}(s)} \right)^2 \left[ \left( \frac{K_o}{s} \right)^2 V_{nt}^2(s) + \Delta\phi_{osc}^2(s) \right] \end{aligned}$$

The grouping of the equation emphasizes the effect of reference and divider noise, phase detector gain and oscillator noise and sensitivity.



Actual Results Achieved in a Low Noise Reference Loop

In the following example of a phase lock loop (PLL), efforts were made to employ all the listed design rules.

As the frequency reference loop of the HP 8662A Synthesized Signal Generator (Fig. 14), the loop's function is to filter the high spurious content of a 320-640MHz reference source. The reference source is directly synthesized from multiples of 10MHz, steps in 20MHz steps, and contains -40dBc spurious signals. The loop reduces spurious signals to -100dBc and, as an additional functions, provides 10MHz steps and switches in less than 50µsec.

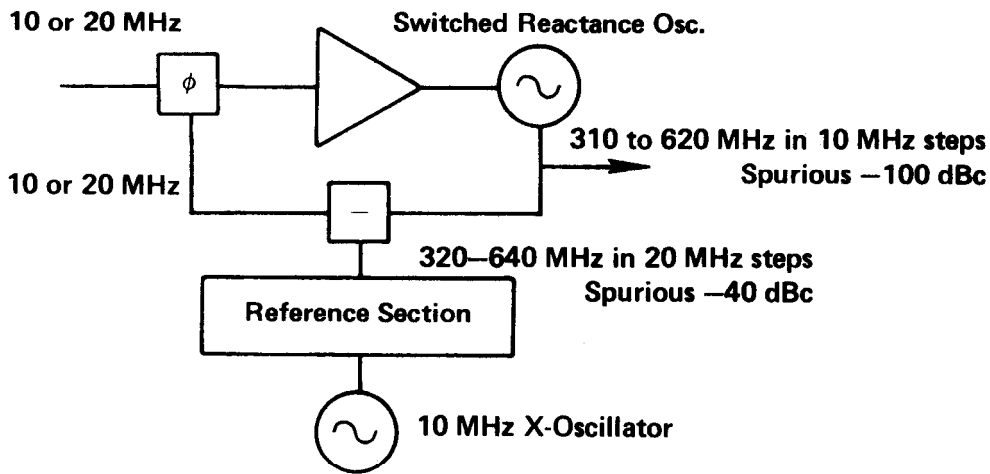


Fig. 14

The 310-620MHz VCO of the loop, also used in a second loop as a 320-640MHz VCO, has a novel switched reactance resonator (Fig. 15). It consists of 5 inductor arrays switched in a binary fashion. They provide 32 frequency steps. For a continuous frequency coverage, the varactor has to cover only 10MHz intervals. Compared to a conventional VCO with a varactor covering the entire 310 to 620MHz range, this switched scheme results in drastically reduced oscillator sensitivity.

The nature of the resonator also allows very high signal levels ( $\pm 10V_{\text{peak}}$ ), high Q (150-250), fast switching, and precise pretuning.

### 310–640 MHz Switched Reactance Oscillator

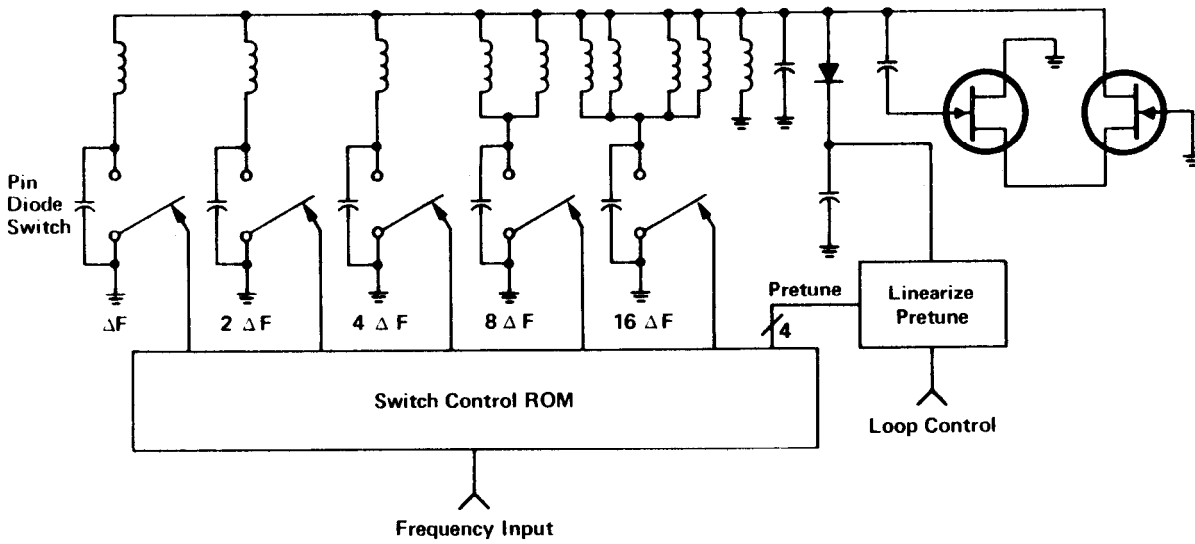


Fig. 15

This loop achieves a noise floor of -143dBc as close in as 10kHz. Within 10kHz, noise of the reference section is dominant.

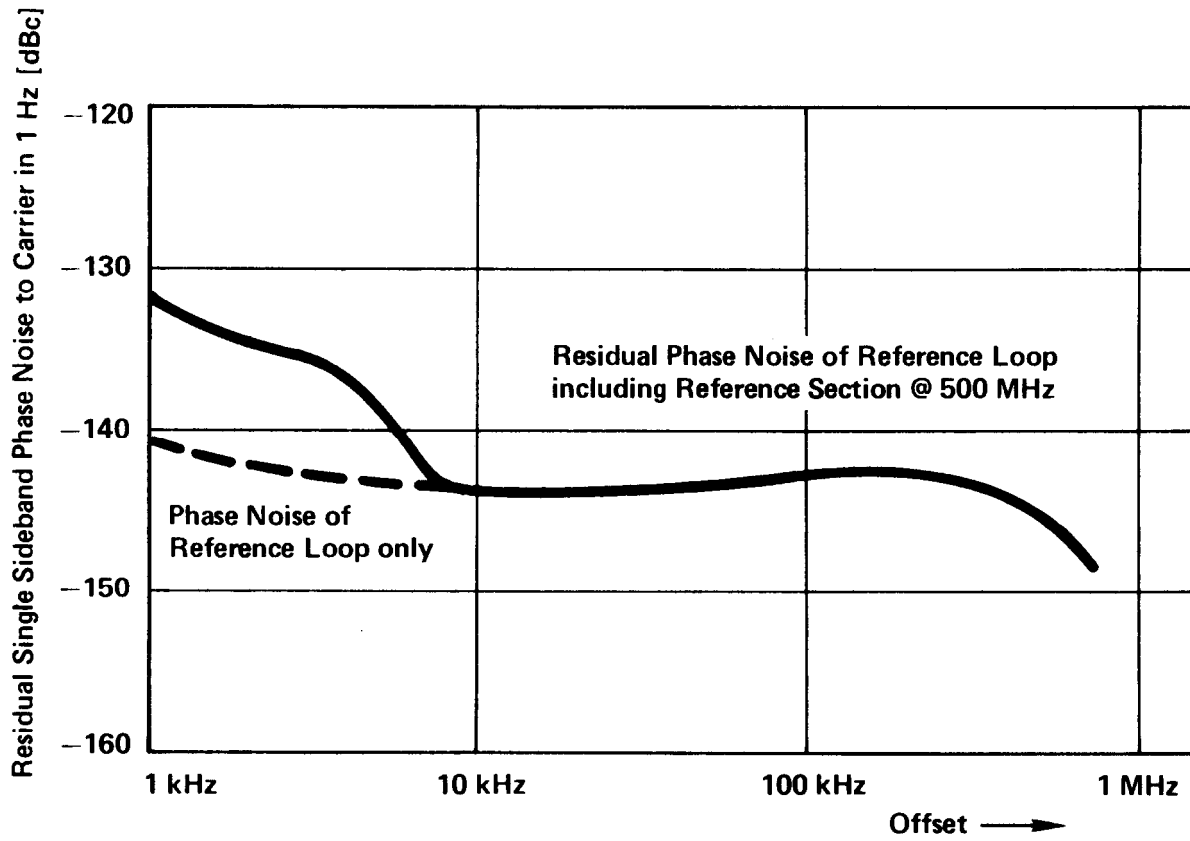


Fig. 16

### Reference Multiplication

Synthesized sources use a reference oscillator - typically a 5 or 10MHz X-oscillator with excellent short and long term stability. To arrive at low phase noise signals in the RF and microwave range the most crucial factor is how the reference signal is multiplied into the RF range.

Fig. 17 compares 3 methods of obtaining a low phase noise 640MHz signal starting with a 10MHz crystal oscillator.

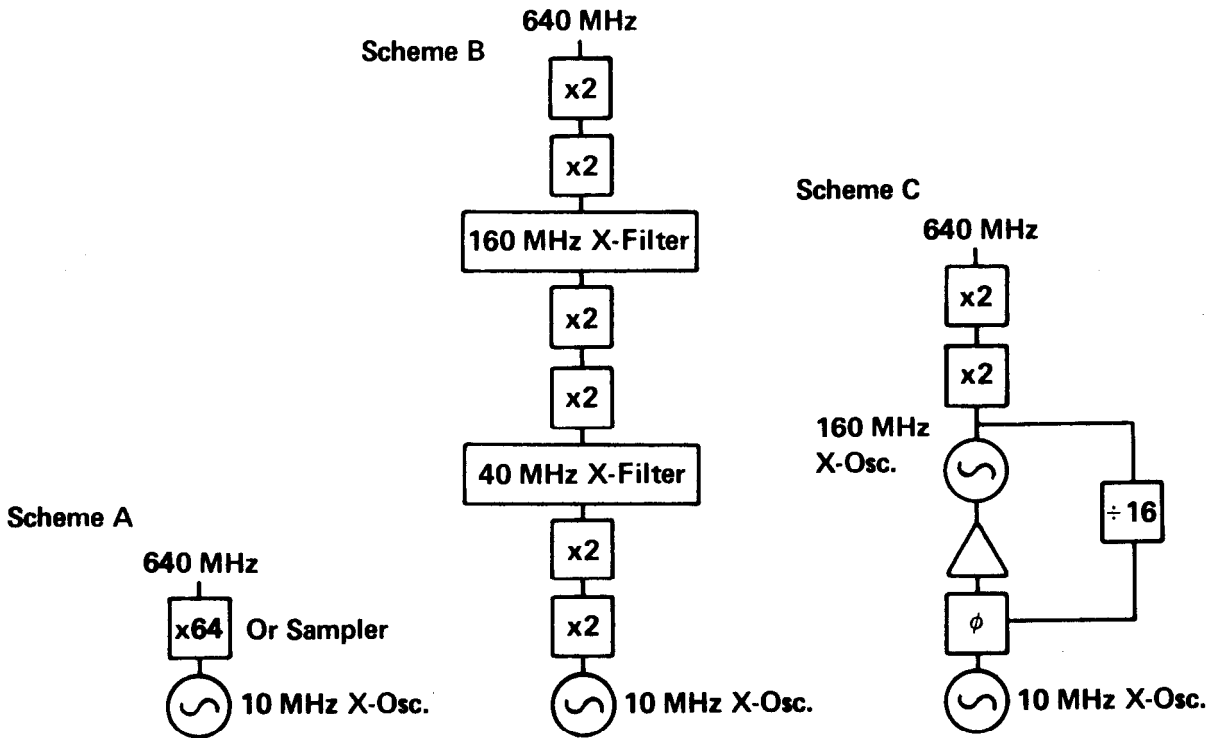


Fig. 17

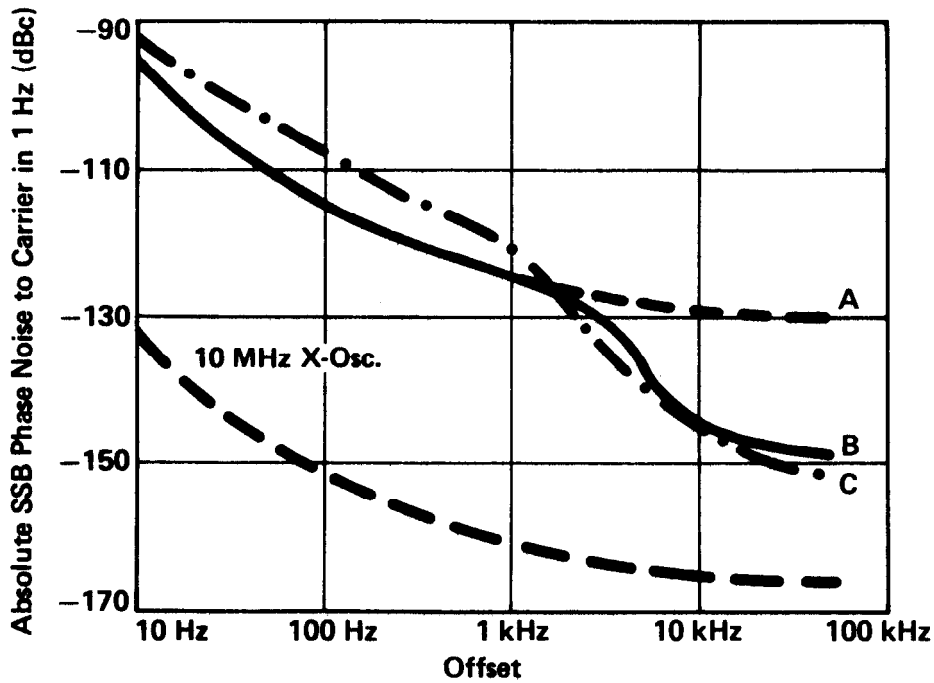


Fig. 18

Method A results in straight multiplication of the reference phase noise. Multiplication can be done by doubling six times or multiplying with a higher order multiplier or sampler. Reference oscillator noise is increased by 36dB. Method B is also straight multiplication, but at appropriate frequency levels (40 and 160MHz), narrow band crystal filters are used to reduce sideband noise. Method C employs a 160MHz crystal oscillator to achieve a low phase noise floor. It is locked to the 10MHz crystal oscillator. As previously discussed, the bandwidth of the loop is determined by comparing the phase noise of the free-running 160MHz crystal oscillator with noise of the reference oscillator and divider noise multiplied by 16. As plot C indicates, divider noise dominates in this case, resulting in higher close-in noise with scheme C than with any of the other schemes.

The HP 8662A Synthesized Signal Generator uses method B. Potential problems of this approach are:

- Additive noise in the first stages of multiplication.
- Low frequency device noise and power supply noise, causing phase modulation in amplifiers, most sensitive again in the first stages of multiplication.
- Doubler noise.
- Crystal filter noise.
- Microphonic noise inducing phase noise in crystal filters.

### Overall Phase Noise Performance of a Synthesized Signal Generator System

So far, circuits and modules have been optimized for low phase noise. They form the building blocks for synthesizers. The particular examples used earlier are part of the new HP 8662A Synthesized Signal Generator. The graph of Fig. 19 below shows the typical residual single sideband phase noise of the system. Below 10kHz, phase noise of the reference section dominates. From 10 to 500 kHz the reference loop and sum loop determine the phase noise performance. Farther out the sum loop oscillator is the dominant phase noise source.

The 8662A system is compared with an older synthesizer design of significantly different structure, the 8660C/86602A. It covers the same frequency range, but was not designed with low phase noise as a primary objective. The HP 8640B cavity-tuned generator is also included, showing excellent phase noise performance at 20kHz offset and farther out. Of course, it cannot compete close-in with synthesized generators.

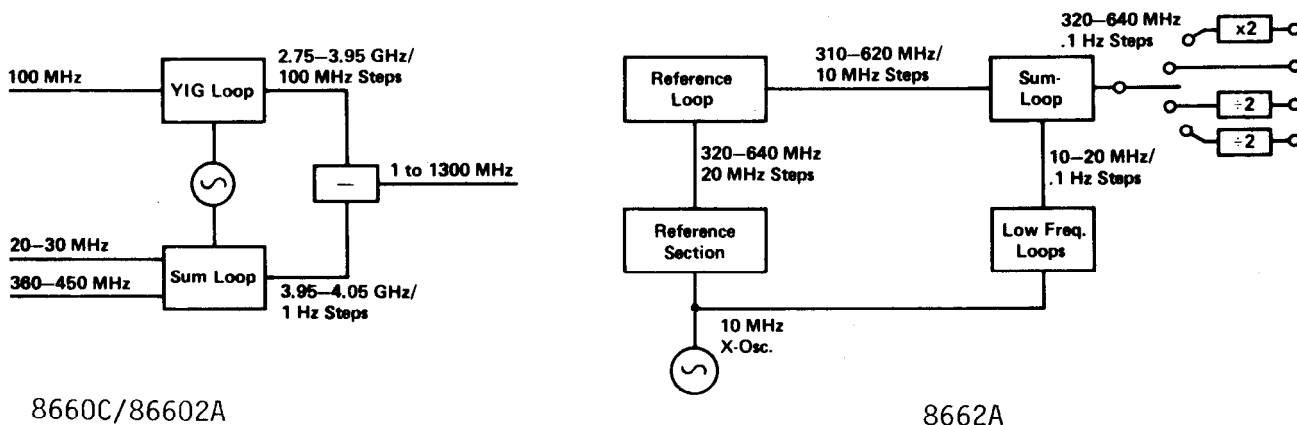


Fig. 19

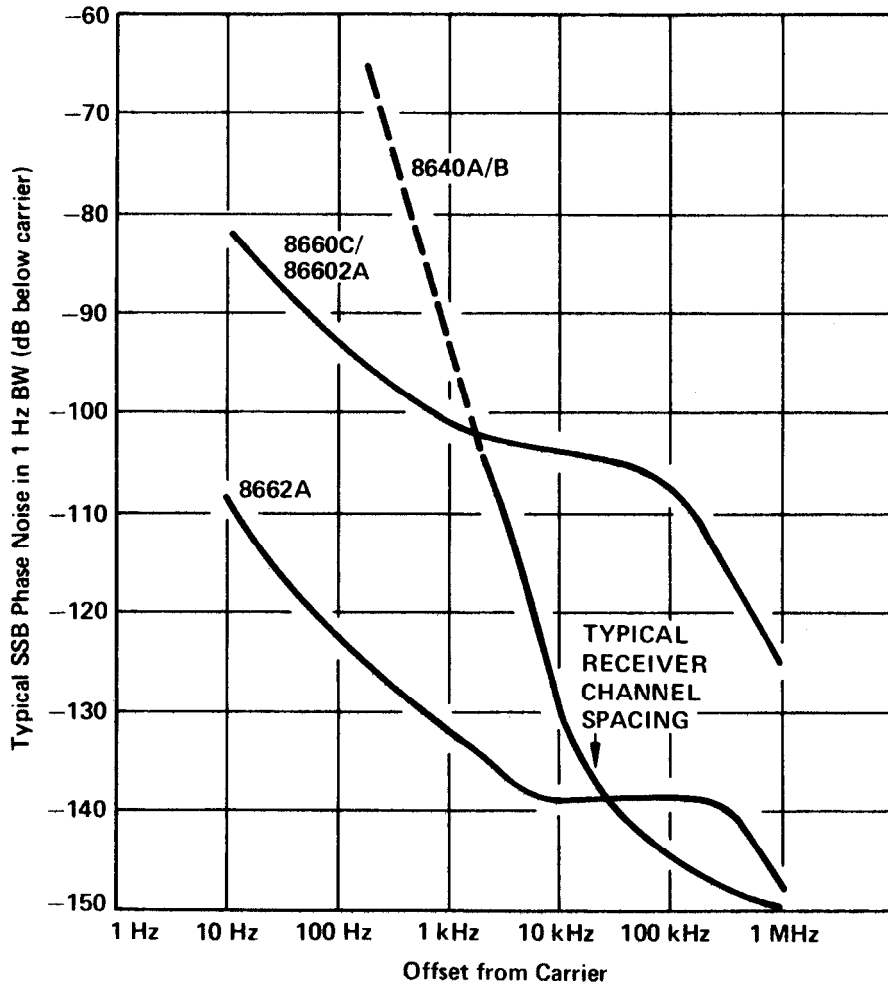


Fig. 20

The overall result of the preceding design considerations is a synthesizer with not only exceptional close-in noise performance, but also very low phase noise at farther-out offset frequencies where traditionally cavity oscillators were far superior. With a switching speed of 500 $\mu$ sec (RF settling) the HP8662A also combines the usually conflicting requirements of low phase noise with high frequency agility.

Measurement of Phase Noise

The emphasis on low phase noise sources in this paper also guides the selection of test methods. Phase noise measurement techniques will be compared on the basis of minimum phase noise  $\mathcal{L}$  measureable.

Heterodyne Frequency Measurement Technique

In the time domain, frequency stability is measured with period counters. Given a stable reference source, the resolution is greatly enhanced by heterodyning.

**Resolution:**  $\frac{\Delta f}{f_o} = \frac{f_D^2 \Delta \tau}{f_o}$

$\frac{\Delta f}{f_o}$  = minimum fractional frequency difference

$f_D$  = difference frequency

$\tau$  = sample time, minimum  $\tau = \frac{1}{f_D}$

$\Delta \tau$  = least digit of period count

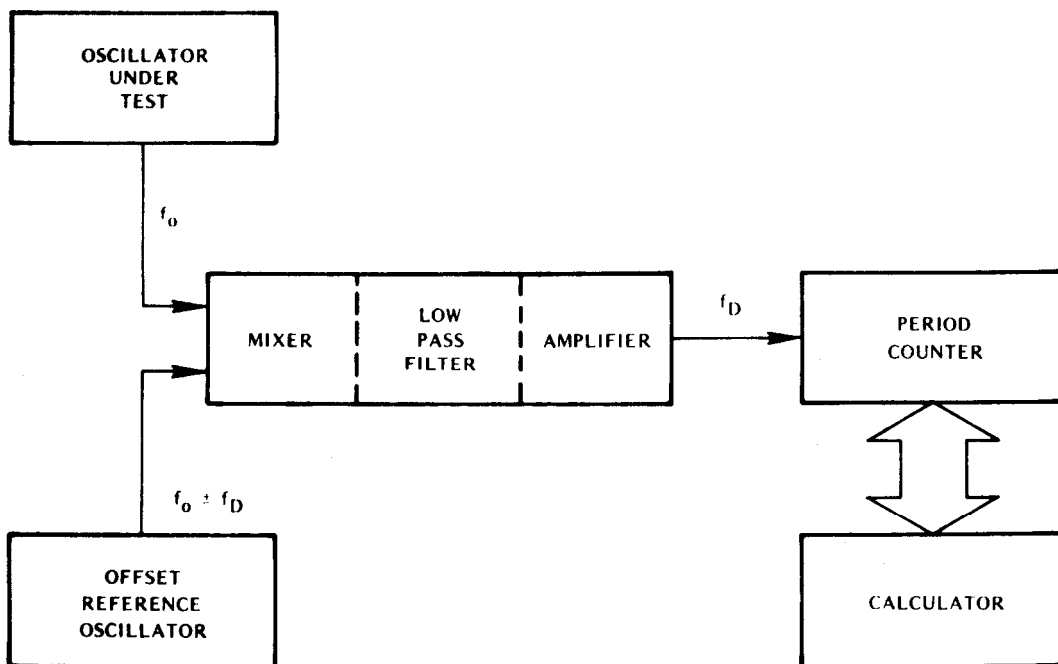


Fig. 21



With computing counters  $\mathcal{L}$  can be obtained conveniently. Desktop computer-based systems like the HP 5390A Frequency Stability Analyzer, convert time domain data into spectral densities. The system noise floor is given by:

$$\mathcal{L}_{\text{system}} = -173 + \log \frac{f_D^2}{f_m} \quad [\text{dBc/Hz}]$$

For example: @  $f_m = 1\text{Hz}$  with  $f_D = 10\text{Hz}$  the system can measure down to  $-153\text{dBc}$ . Compared with other methods this technique loses its advantage quickly above Fourier frequencies greater than  $100\text{Hz}$ .

### Phase Noise Measurement with Spectrum Analyzer

RF spectrum analyzers measure the spectral density  $\mathcal{L}$  directly, provided that the phase noise of the source under test is significantly above its AM noise.

By down converting with a clean reference source, AM noise of the source under test can be suppressed if it is used as the high level LO drive for the mixer.

Limitations of this direct method are phase noise of the spectrum analyzer LO, dynamic range and resolution.

An RF spectrum analyzer with a YIG oscillator as LO can measure  $\mathcal{L}$  @  $100\text{kHz}$  down to approximately  $-120\text{dBc}$ . Spectrum analyzers with synthesized LO allow phase noise measurements closer in.

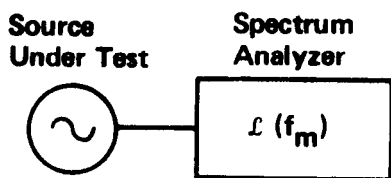


Fig. 22

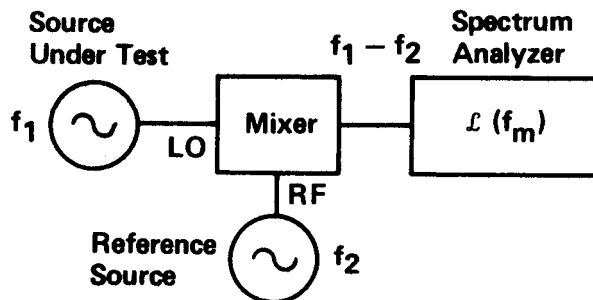


Fig. 23

Phase Noise Measurement with Frequency Discriminator

The spectral density of frequency fluctuations  $S_{\Delta f}(f_m)$  of the source under test is obtained when the signal is applied to a frequency discriminator either directly or in a heterodyne fashion.

$$\Delta f_{rms} = \frac{1}{K_F} \Delta V_{rms}$$

$$S_{\Delta f}(f_m) = \frac{1}{K_F^2} (\Delta V_{rms})^2 (1 \text{ Hz})$$

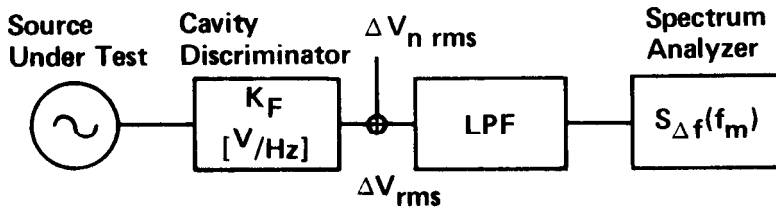


Fig. 24

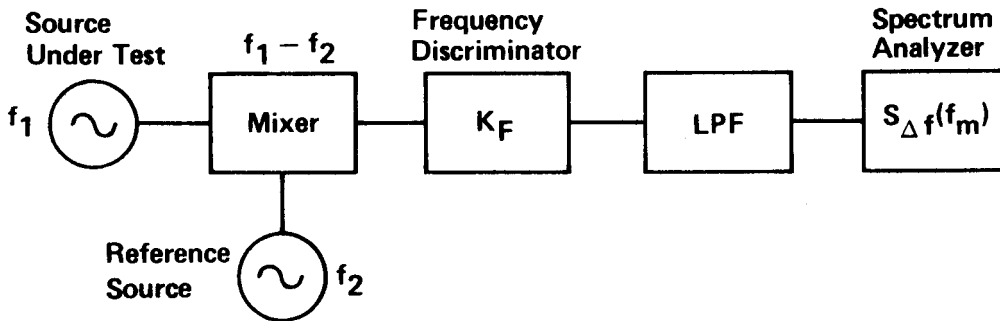


Fig. 25

$\mathcal{L}(f_m)$  is calculated from  $S_{\Delta f}$   $\mathcal{L}(f_m) = \frac{1}{2} \frac{1}{f_m^2} S_{\Delta f}(f_m)$

Assuming a noise floor of the discriminator represented by  $\Delta V_{n\text{ rms}}$ , the system noise for  $\mathcal{L}(f_m)$  is

$$\mathcal{L}_{\text{system}}(f_m) = \frac{1}{2} \frac{1}{K_F^2} \frac{1}{f_m^2} (\Delta V_{n\text{ rms}})^2 (1\text{ Hz})$$

It indicates the basic drawback of the use of the frequency discriminator method in determining phase noise  $\mathcal{L}(f_m)$  of a source. The system's noise floor rises with  $f_m^{-2}$  towards low offsets. This assumes a white spectrum of  $\Delta V_n$ .

Using the 8901A modulation analyzer ( $\Delta f_{\text{res}} = .5\text{Hz}$ ), for example, as the frequency discriminator,  $\mathcal{L}_{\text{system}} @ 1\text{kHz}$  will be  $-105\text{dBc}$ .

Delay Line and Mixer as Frequency Discriminator

A mixer operating as a phase detector and a delay line have the combined effect of a frequency discriminator yielding again  $S_{\Delta f}(f_m)$ .

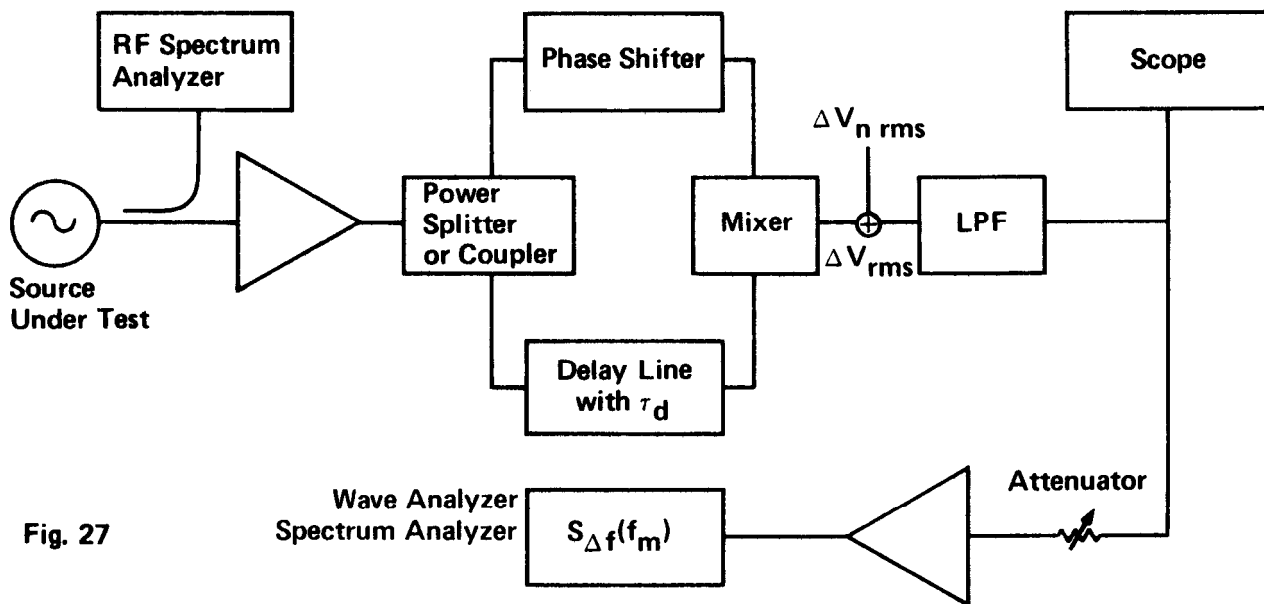


Fig. 27

Fig. 26

Both inputs to the mixer have to be in quadrature to assure maximum phase sensitivity.

The output voltage  $\Delta V$  of the mixer is proportional to the frequency deviation  $\Delta f$  of the source, to the phase detector constant  $k_\phi$  and has a periodic  $\left(\frac{\sin x}{x}\right)$  dependence on  $f_m \tau_d$ .

$$\Delta V = K_\phi \Delta \phi$$

$$\Delta V = K_\phi \tau_d \frac{\sin\left(\frac{\omega_m \tau_d}{2}\right)}{\frac{\omega_m \tau_d}{2}} \times \Delta \omega$$

$\tau_d = \text{Delay Time}$   
 $k_\phi = \text{Phase Detector Constant}$   
 $= V_{\text{beat, peak}}$  for sinusoidal beat signal

for  $f_m \ll \frac{1}{2\tau_d}$

$$\Delta f_{\text{rms}} = \frac{\Delta V_{\text{rms}}}{2\pi k_\phi \tau_d} \quad \mathcal{L}(f_m) = \frac{1}{2f_m^2} \quad S_{\Delta f}(f_m) = \frac{1}{2} \frac{(\Delta V_{\text{rms}})^2 (1 \text{ Hz})}{(2\pi)^2 k_\phi^2 \tau_d^2 f_m^2}$$

$$S_{\Delta f}(f_m) = \frac{(\Delta V_{\text{rms}})^2 (1 \text{ Hz})}{(2\pi)^2 k_\phi^2 \tau_d^2}$$

The sensitivity of the system can again be evaluated by replacing  $\Delta V_{\text{rms}}$  caused by frequency fluctuations of the source with  $\Delta V_{n \text{ rms}}$  representing mixer noise plus noise of the following amplifier.

$$\mathcal{L}_{\text{system}}(f_m) = \frac{1}{2} \frac{(\Delta V_{n \text{ rms}})^2 (1 \text{ Hz})}{(2\pi)^2 k_\phi^2 \tau_d^2 f_m^2}$$

With white mixer (+ amplifier) noise the system sensitivity decreases with  $f_m^{-2}$ . Flicker characteristic of the mixer noise causes the noise floor to rise with  $f_m^{-3}$  towards low offsets.

Reference [6], [7] explores this method extensively.  $\mathcal{L}_{\text{system}}$  @ 1kHz can be as low as -115dBc.

Phase Noise Measurement with Two Sources and Phase Detector

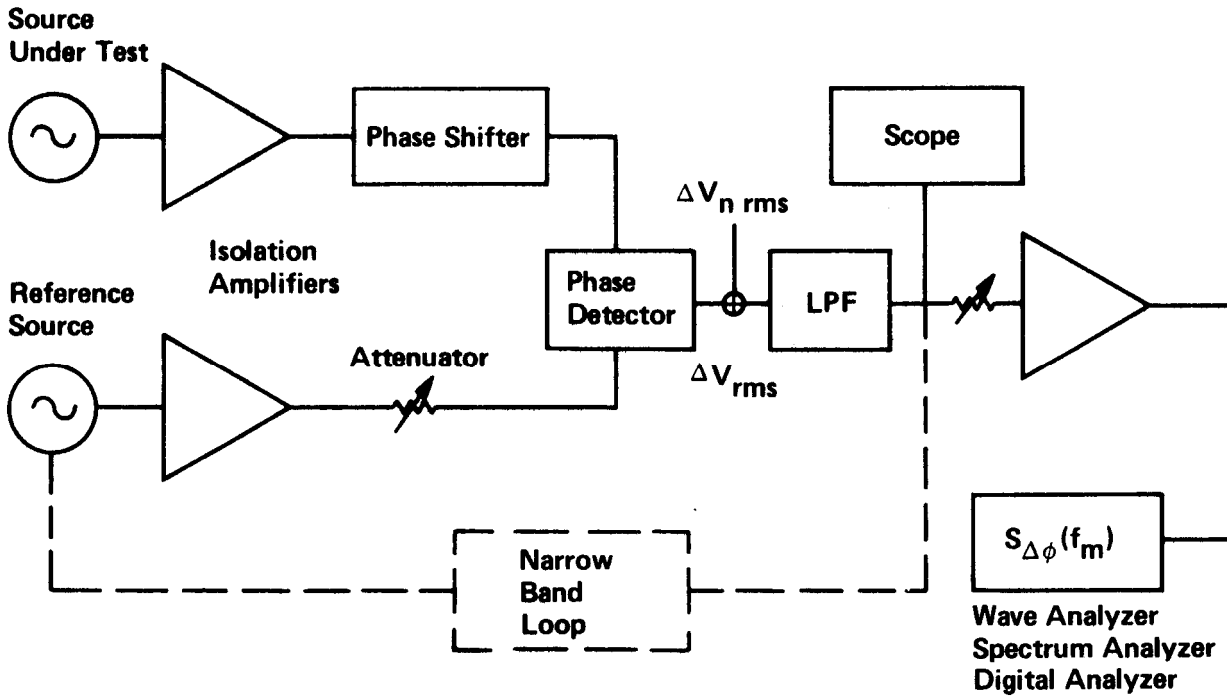


Fig. 27

The most direct and also most sensitive method to measure the spectral density of phase noise  $S_{\Delta\phi}(f_m)$  requires 2 sources - one or both of them may be the device(s) under test - and a double balanced mixer used as a phase detector. The RF and LO input to the mixer should be in phase quadrature indicated by  $0\ V_{DC}$  at the IF port. Good quadrature assures maximum phase sensitivity  $k\phi$  and minimum AM sensitivity. With a linearly operating mixer,  $k\phi$  equals the peak voltage of the sinusoidal beat signal produced when both sources are frequency offset.

When both signals are set in quadrature, the voltage  $\Delta V$  at the IF port is proportional to the fluctuating phase difference between the two signals.

$$\Delta \phi_{rms} = \frac{1}{k_{\phi}} V_{rms}$$

$k_{\phi}$  = Phase detector constant

$$S_{\Delta \phi}(f_m) = \frac{(\Delta V_{rms})^2(1 \text{ Hz})}{V_{B \text{ peak}}^2} = \frac{1}{2} \frac{(\Delta V_{rms})^2(1 \text{ Hz})}{V_{B \text{ rms}}^2}$$

=  $V_{B \text{ peak}}$  for sinusoidal beat signal

$$L(f_m) = \frac{1}{2} S_{\Delta \phi}(f_m) = \frac{1}{4} \frac{(\Delta V_{rms})^2(1 \text{ Hz})}{V_{B \text{ rms}}^2}$$

The calibration of the wave analyzer or spectrum analyzer can be read from the above equations. For a plot of  $L(f_m)$  the 0 dB reference level is to be set 6dB above the level of the beat signal. The -6dB offset has to be corrected by +1.0dB for a wave analyzer and by +2.5dB for a spectrum analyzer with log amplifier and average detector. In addition, noise bandwidth corrections may have to be applied.

Since the phase noise of both sources is measured in this system, the phase noise performance of one of them needs to be known for definite data on the other source. Frequently it is sufficient to know that the actual phase noise of the dominant source can not deviate more than 3dB from the measured data. If 3 unknown sources are available, 3 measurements with 3 different source combinations yield sufficient data to calculate accurately each individual performance.

Fig. 27 indicates a narrow band phase lock loop which maintains phase quadrature for sources which are not sufficiently phase stable over the period of the measurement. The two isolation amplifiers should prevent injection locking of the sources.

Residual phase noise measurements test one or two devices like amplifiers, dividers (Fig. 11), synthesizers (Fig. 29), driven by one common source. Since this source is not phase noise free, it is important to know the degree of cancellation as function of Fourier frequency.

The noise floor of the system is established by the equivalent noise voltage  $\Delta V_n$  at the mixer output. It represents mixer noise as well as the equivalent noise voltage of the following amplifier.

$$L_{\text{system}}(f_m) = \frac{1}{4} \frac{(\Delta V_{n \text{ rms}})^2 (1 \text{ Hz})}{V_B^2 \text{ rms}}$$

Noise floors close to -180dBc can be achieved with a high level mixer and low noise port amplifier. The noise floor increases with  $f_m^{-1}$  due to the flicker characteristic of  $\Delta V_n$ . System noise floor of -166dBc @ 1kHz have been realized.

In measuring low phase noise sources a number of potential problems have to be understood to avoid erroneous data:

- If two sources are phase locked to maintain phase quadrature, it has to be insured that the lock bandwidth is significantly lower than the lowest Fourier frequency of interest.
- Even with no apparent phase feedback, 2 sources can be phase locked -injection locked- resulting in suppressed close-in phase noise.
- AM noise of the RF signal can come through if the quadrature setting is not maintained sufficiently.
- Deviation from the quadrature setting will also lower the effective phase detector constant.
- Non-linear operation of the mixer results in a calibration error.
- A non-sinusoidal RF signal causes  $k\phi$  to deviate from  $V_B \text{ peak}$ .
- The amplifier or spectrum analyzer input can be saturated during calibration or by high spurious signals like line frequency multiples.

- Closely spaced spurious such as multiples of 60Hz may give the appearance of continuous phase noise when insufficient resolution and averaging is used on the spectrum analyzer.
- Impedance interfaces should remain unchanged going from calibration to measurement.
- In residual measurement systems phase noise of the common source might be insufficiently cancelled due to improperly high delay time differences between the two branches.
- Noise from power supplies for devices under test or the narrow band phase lock loop can be a dominant contributor of phase noise.
- Peripheral instrumentation like the oscilloscope, analyzer, counter, DVM, can inject noise.
- Microphonic noise might excite significant phase noise in devices.

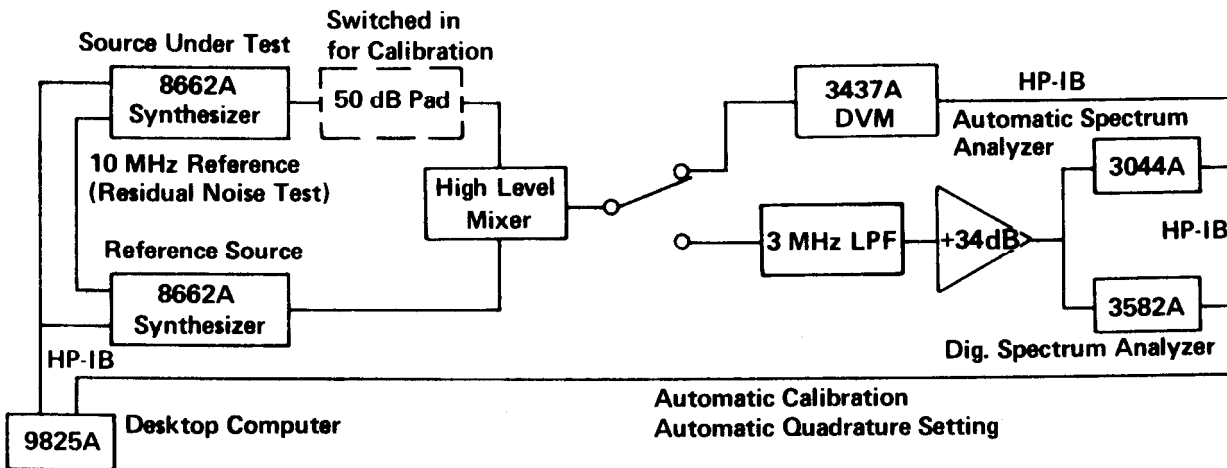


Fig. 28



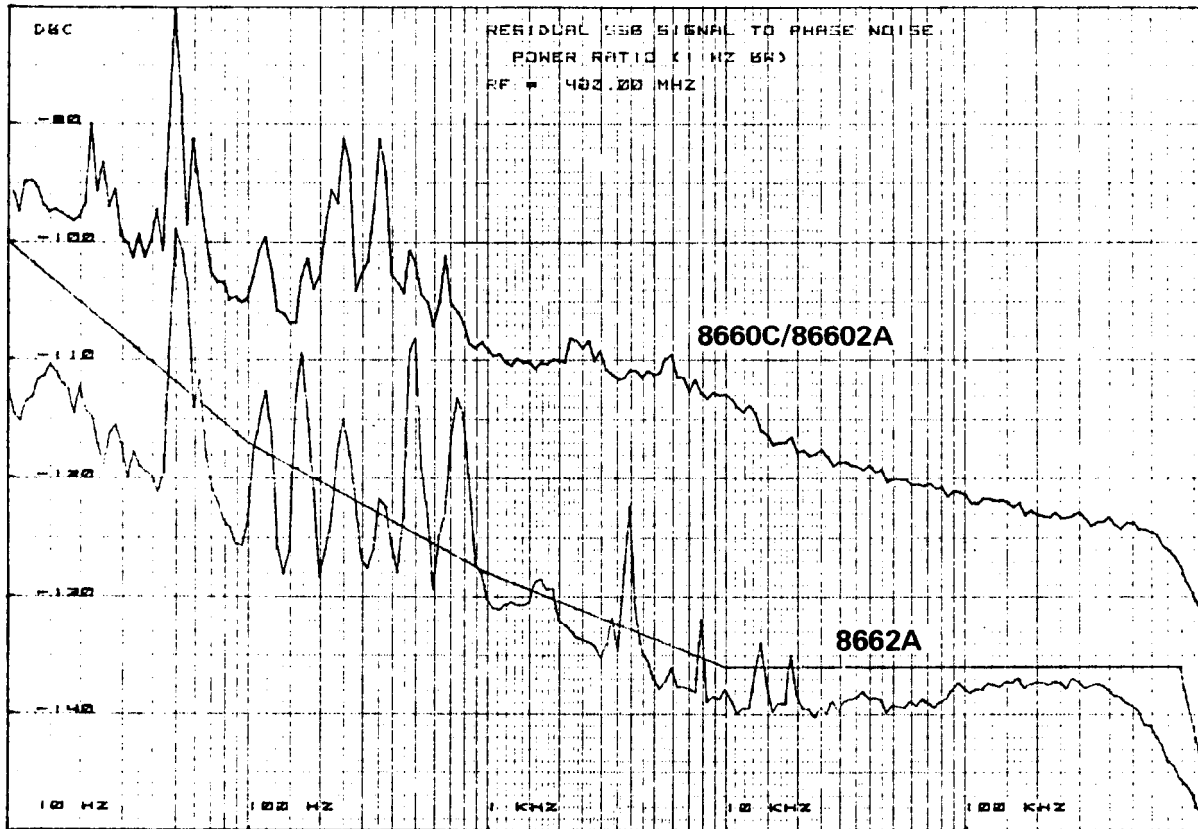


Fig. 29

Despite all of these hazards, automatic test systems have been developed and operated successfully. [Ref. 6] Fig. 28 shows a system which measures automatically the residual phase noise of the 8662A Synthesizer. It is a residual test since both instruments use one common 10MHz reference x-oscillator. Quadrature setting is conveniently controlled by probing the beat signal with a digital voltmeter and stopping the phase advance of one synthesizer when the beat signal voltage is sufficiently close to 0.

The two plots of Fig. 29 were done with the 3044A Automatic Spectrum Analyzer covering 10Hz to 13MHz. The test system also measures spurious signals. They appear rather broad on this chart due to a limited number of data points per decade. Again, the older 8660C/86602A Synthesized Signal Generator is compared with the new 8662A.

Acknowledgement

The author thanks Skip Crilly, Howard Swain, Roger Muat, John Richardson and John Minck for helpful discussions and comments. Of special value were the shared experiences of Bill Chan on reference multiplication, Fred Ives on phaselock loops and Roland Hassun, Project Manager of the HP8662A.

Glossary of Symbols

$A(s)$	Transfer function of amplifier
$B$	Bandwidth
$FkTB$	Available noise power in bandwidth $B$
$f_o$	Carrier frequency
$f_c$	Corner frequency of flicker noise
$f_m$	Fourier frequency (sideband-, offset-, modulation, baseband-frequency)
$f(t)$	Instantaneous frequency
$\Delta f(t)$	Instantaneous frequency fluctuation
$\Delta f_{peak}$	Peak deviation of sinusoidal frequency modulation
$\Delta f_{res}$	Residual FM
$G_{ol}(s)$	Open loop gain of phase lock loop
$K_a (s)$	Transfer function of attenuator
$K_o$	Gain constant of voltage tunable oscillator
$K_s$	Shaper constant
$K_\phi$	Phase detector gain
$\mathcal{L}(f_m)$	Single sideband phase noise to total signal power in a 1 Hz bandwidth
$P_s$	Signal power
$P_{ssB}$	Power of single sideband
$P_{s av}$	Available signal power
$Q_{unl}$	Quality factor of unloaded resonator
$s$	Complex frequency
$S_{\Delta f}(f_m)$	Spectral density of frequency fluctuations
$S_y(f_m)$	Spectral density of fractional frequency fluctuations
$S_{\Delta\theta}(f_m)$	Spectral density of phase perturbation
$S_{\Delta\phi}(f_m)$	Spectral density of phase noise
$t$	Time variable
$v(t)$	Instantaneous voltage
$V_{sL}$	Peak amplitude of sinusoidal signal at limiting port
$V_{n rms}$	Equivalent noise voltage (1 Hz bandwidth)
$V_{s av}$	Available signal voltage
$W_e$	Maximum energy stored in capacitor
$y(t)$	Instantaneous fractional frequency offset from nominal frequency
$\Delta\theta(t)$	Instantaneous fluctuation of phase perturbation
$\sigma_y^2(\tau)$	Allan variance
$\tau$	Sample time
$\Delta\phi(t)$	Instantaneous phase fluctuation
$\Delta\phi_{peak}$	Peak deviation of sinusoidal phase modulation, also modulation index
$\omega$	Angular frequency

## References

- x 1) Barnes, J.A. Chie, A. R., Cutter, L.S., et al, "Characterization of Frequency Stability", IEEE Trans. on Instr. and Meas. IM-20, No. 2, pp. 105-120, May 1971.
- 2) Fischer, M. C., "Frequency Stability Measurement Procedures", Eighth Annual Precise Time and Time Interval Applications and Planning Meeting, Dec. 1976.
- 3) D. J. Healey, III, "Flicker of Frequency and Phase and White Frequency and Phase Fluctuations in Frequency Sources," Proc. 26th Annual Symp. on Freq. Control, Fort Monmouth, N. J., pp. 43-49, June 1972.
- 4) Hewlett-Packard staff, "Understanding and Measuring Phase Noise in the Frequency Domain," Application Note 207, October 1976.
- 5) Howe, D.A., "Frequency Domain Stability Measurements: A Tutorial Introduction" NBS Technical Note 679, March 1976.
- 6) Lance, A.L., Seal, W.D. Mendoza, F. G. and Hudson, N.W., "Automating Phase Noise Measurements in the Frequency Domain", Proc. of the 31st Annual Symposium on Frequency Control, June 1977.
- 7) Lance, A.L., Seal, W.D., Hudson, N.W., Mendoza, F. G., and Donald Halford, "Phase Noise Measurements Using Cross-Spectrum Analysis," Conference on Precision Electromagnetic Measurements, Ottawa, Canada, June 1978
- \* 8) Leeson, D.B., "A Simple Model of Feedback Oscillator Noise Spectrum," Proc. IEEE L, Vol. 54, pp. 329-330, February 1966.
- \* 9) Sauvage, G., "Phase Noise in Oscillators: A Mathematical Analysis of Leeson's Model", IEEE Trans. on Instr. and Meas., Vol IM-26, No. 4, Dec. 1977.
- 10) Shoaf, J. H., Halford, D., Risley, A.S., "Frequency Stability Specification and Measurement: High Frequency and Microwave Signals", NBS Technical Note 632, Jan. 1973.